Supplement of Atmos. Chem. Phys., 25, 18355–18371, 2025
https://doi.org/10.5194/acp-25-18355-2025-supplement

Atmospheric Chemistry and Physics
Open Access
EGU

Supplement of

The critical role of oxygenated volatile organic compounds (OVOCs) in shaping photochemical O_3 chemistry and control strategy in a subtropical coastal environment

Lirong Hui et al.

Correspondence to: Zhe Wang (z.wang@ust.hk)

Table S1. The LOD and R^2 of the calibrated compounds measured by PTR-ToF-MS.

Compounds	Protonated mass (m/z)	Empirical formula	LOD (ppbv)	R^2
Methanol	33.034	CH_4OH^+	0.094	0.998
Acetonitrile	42.034	$C_2H_3NH^+$	0.037	0.991
Propylene	43.054	$C_3H_6H^+$	0.077	0.993
Acetaldehyde	45.033	$C_2H_4OH^+$	0.052	0.995
Acrolein	57.034	$C_3H_4OH^+$	0.014	0.990
Acetone	59.049	$C_3H_6OH^+$	0.057	0.996
Dimethyl sulfide (DMS)	63.026	$C_2H_6SH^+$	0.011	0.996
Isoprene	69.07	$C_5H_8H^+$	0.023	0.996
3-buten-2-one (MVK)	71.049	$C_4H_6OH^+$	0.038	0.994
Butan-2-one	73.065	$C_4H_8OH^+$	0.022	0.995
Benzene	79.054	$C_6H_6H^+$	0.012	0.995
Ethyl Acetate	89.06	$C_4H_8O_2H^+$	0.016	0.994
Toluene	93.07	$C_7H_8H^+$	0.021	0.994
Methyl Butyl Ketone, Methyl Isobutyl Ketone	101.096	$C_6H_{12}OH^+$	0.016	0.994
Styrene	105.07	$C_8H_8H^+$	0.010	0.997
m-xylene	107.086	$C_8H_{10}H^+$	0.010	0.994
1,2,4-trimethylbenzene	121.101	$C_9H_{12}H^+$	0.015	0.992
Naphthalene	129.07	$C_{10}H_8H^+$	0.014	0.998
Alpha-pinene, +3-carene	137.132	$C_{10}H_{16}H^+$	0.009	0.994

Table S2. The average concentrations of VOC species measured by PTR-ToF-MS in summer, autumn, and early winter.

Compound	Ion formula	m/z	Summer average concentration (ppbv)	Autumn average concentration (ppbv)	Early winter average concentration (ppbv)
BVOCs					
Isoprene, fragmentation	$C_5H_8^*$	69.07	1.571	0.587	0.404
Monoterpenes	$C_{10}H_{16}^*$	137.132	0.276	0.156	0.103
AVOCs					
Propenes	C_3H_6	43.054	0.166	0.174	0.173
Butenes	C_4H_8	57.07	0.747	1.348	1.346
Cyclopentadiene	C_5H_6	67.054	0.056	0.038	0.030
Pentenes	C_5H_{10}	71.086	0.198	0.271	0.272
Benzene, Ethylbenzene fragment	$C_6H_6^*$	79.054	0.228	0.754	0.925
Methylcyclopentane	C_6H_{10}	83.085	0.256	0.243	0.216
Hexenes	C_6H_{12}	85.101	0.043	0.078	0.076
Toluene	$C_7H_8^*$	93.07	0.572	1.664	1.871

C_7 cycloalkanes	C_7H_{12}	97.101	0.119	0.122	0.105
Styrene	$C_8H_8^*$	105.07	0.027	0.086	0.079
C_8 aromatics	$C_8H_{10}^*$	107.086	0.476	1.423	1.390
C_2 cyclohexanes	C_8H_{14}	111.117	0.084	0.074	0.064
C_9 aromatics	$C_9H_{12}^*$	121.1012	0.105	0.217	0.184
Naphthalene	$C_{10}H_8$	129.07	0.111	0.155	0.147
Tetrahydronaphthalene	$C_{10}H_{12}$	133.101	0.017	0.036	0.036
C_{10} Aromatics	$C_{10}H_{14}$	135.117	0.065	0.144	0.131
C_{11} aromatics	$C_{11}H_{16}$	149.132	0.023	0.040	0.032
Biphenyl, Acenaphthene	$C_{12}H_{10}$	155.086	0.016	0.034	0.036
C2 naphthalene	$C_{12}H_{12}$	157.101	0.025	0.035	0.034
C_{12} aromatics	$C_{12}H_{18}$	163.148	0.014	0.022	0.016
C_3 naphthalene	$C_{13}H_{14}$	171.117	0.016	0.026	0.026
C_{13} aromatics	$C_{13}H_{20}$	177.164	0.018	0.018	0.011
Anthracene	$C_{14}H_{10}$	179.086	0.003	0.005	0.006
C_{14} aromatics	$C_{14}H_{22}$	191.18	0.014	0.014	0.010
$C_xH_yO_1$					
Methanol	CH_4O^*	33.034	5.978	9.216	10.097
Acetaldehyde	$C_2H_4O^*$	45.033	1.849	3.526	3.859
Acrolein	$C_3H_4O^*$	57.034	0.900	0.829	0.811
Acetone, Propanal	$C_3H_6O^*$	59.049	4.221	5.386	5.670
Furan	C_4H_4O	69.034	0.021	0.046	0.057
Methyl Vinyl Ketone (MVK), Methacrolein (MACR), Crotonaldehyde	$C_4H_6O^*$	71.049	0.357	0.347	0.312
Methyl ethyl ketone (MEK), Butanal, 2-methylpropanal	$C_4H_8O^*$	73.065	0.691	1.470	1.672
Methyl furan	C_5H_6O	83.049	0.058	0.078	0.077
C_5 ketones, Cyclopentanone	C_5H_8O	85.065	0.108	0.148	0.168
Pentanal, Pentanones	$C_5H_{10}O^*$	87.08	0.147	0.212	0.251
Phenol	$C_6H_6O^*$	95.049	0.054	0.062	0.065
C_2-substituted furans	C_6H_8O	97.065	0.040	0.056	0.063
Hexenals, Cyclohexanone, Hexenones	$C_6H_{10}O^*$	99.08	0.152	0.386	0.403
Hexanal, Hexanone	$C_6H_{12}O^*$	101.096	0.049	0.051	0.055
Benzaldehyde	$C_7H_6O^*$	107.049	0.071	0.118	0.125
Cresols	$C_7H_8O^*$	109.065	0.094	0.096	0.096
C_3-substituted furans	$C_7H_{10}O$	111.08	0.036	0.043	0.043
Cycloheptanone	$C_7H_{12}O$	113.096	0.033	0.059	0.067
Heptanal	$C_7H_{14}O^*$	115.112	0.022	0.029	0.034
Benzofuran	C_8H_6O	119.049	0.040	0.067	0.077

o-, m- and *p*-Tolualdehydes	$C_8H_8O^*$	121.065	0.062	0.129	0.164
C_2 Phenols	$C_8H_{10}O^*$	123.08	0.017	0.041	0.023
C_4 furan	$C_8H_{12}O$	125.096	0.018	0.028	0.032
Cyclooctanone	$C_8H_{14}O$	127.111	0.039	0.025	0.027
Octanal	$C_8H_{16}O$	129.127	0.039	0.070	0.087
Methyl benzofurans	C_9H_8O	133.065	0.016	0.032	0.028
C_3 Phenols	$C_9H_{12}O^*$	137.096	0.015	0.028	0.023
Nopinone	$C_9H_{14}O^*$	139.112	0.045	0.078	0.071
Ethenyl benzofuran	$C_{10}H_8O$	145.065	0.009	0.018	0.020
Dimethylbenzofuran	$C_{10}H_{10}O$	147.08	0.010	0.030	0.030
Methyl chavicol	$C_{10}H_{12}O$	149.096	0.010	0.021	0.024
C_4 Phenols	$C_{10}H_{14}O$	151.112	0.021	0.038	0.037
Camphor	$C_{10}H_{16}O$	153.127	0.022	0.060	0.064
Linalool	$C_{10}H_{18}O$	155.143	0.011	0.016	0.017
Decanal	$C_{10}H_{20}O$	157.159	0.073	0.039	0.021
$C_xH_yO_2$					
Formic acid	$CH_2O_2^*$	47.013	0.190	0.500	0.815
Acetic acid, Glycolaldehyde	$C_2H_4O_2^*$	61.028	1.913	4.727	5.754
Ethane diol	$C_2H_6O_2^*$	63.044	0.095	0.094	0.074
Methylglyoxal, Acrylic acid	$C_3H_4O_2^*$	73.028	0.166	0.135	0.126
Propanoic acid, Hydroxyacetone, Methyl acetate	$C_3H_6O_2^*$	75.044	0.944	1.724	1.858
Propylene glycol	$C_3H_8O_2^*$	77.06	0.084	0.091	0.083
Furanone	$C_4H_4O_2^*$	85.028	0.069	0.094	0.105
Butanedione, Methacrylic acid, Methyl acrylate	$C_4H_6O_2^*$	87.044	0.250	0.385	0.415
Butyric acid, methyl propanoate	$C_4H_8O_2^*$	89.06	0.474	0.969	1.098
Furfural	$C_5H_4O_2$	97.028	0.042	0.077	0.089
Methyl furanone	$C_5H_6O_2^*$	99.044	0.112	0.147	0.150
Methyl methacrylate	$C_5H_8O_2^*$	101.06	0.317	0.314	0.310
Pentanoic acid	$C_5H_{10}O_2^*$	103.075	0.018	0.032	0.029
Methylfurfural, Benzenediol	$C_6H_6O_2^*$	111.044	0.060	0.059	0.054
Dimethyl furanone	$C_6H_8O_2^*$	113.06	0.081	0.100	0.106
C_6 diketone isomers, C_6 esters	$C_6H_{10}O_2^*$	115.075	0.091	0.146	0.168
Butyl ester acetic acid	$C_6H_{12}O_2$	117.091	0.017	0.024	0.027
Salicyladehyde	$C_7H_6O_2$	123.044	0.024	0.083	0.092
Methyl benzoic acid	$C_8H_8O_2^*$	137.06	0.070	0.026	0.041
Eugenol	$C_{10}H_{12}O_2$	165.091	0.007	0.012	0.012
$C_xH_yO_3$					

Peracetic acid	$C_2H_4O_3$*	77.023	0.118	0.296	0.374
Maleic anhydride	$C_4H_2O_3$*	99.008	0.038	0.089	0.131
Dihydro furandione	$C_4H_4O_3$	101.023	0.070	0.092	0.106
Acetic anhydride	$C_4H_6O_3$*	103.039	0.058	0.056	0.054
Methylfurandione	$C_5H_4O_3$*	113.023	0.081	0.109	0.124
C_5 3-oxy 3DBE	$C_5H_6O_3$	115.039	0.043	0.077	0.086
Hydroxy benzoquiunone	$C_6H_4O_3$	125.023	0.026	0.044	0.049
Vanillin	$C_8H_8O_3$	153.055	0.015	0.040	0.040
N/S-containing VOC					
Acetonitrile	C_2H_3N	42.034	0.531	0.357	0.359
Etheneamine	C_2H_5N	44.0495	0.160	0.112	0.088
Formamide	CH_3NO	46.029	0.595	0.584	0.570
Acrylonitrile	C_3H_3N	54.034	0.034	0.068	0.077
Propane nitrile	C_3H_5N	56.049	0.309	0.162	0.119
Hydroxy acetonitrile	C_2H_3NO	58.029	0.084	0.124	0.140
Propene amine	C3H7N	58.065	0.039	0.059	0.056
Acetamide	C_2H_5NO	60.044	0.374	0.527	0.569
Dimethyl sulfide (DMS)	C_2H_6S*	63.026	0.058	0.053	0.054
Pyrrole	C_4H_5N	68.0495	0.028	0.018	0.015
Butane nitrile	C_4H_7N	70.065	0.106	0.072	0.063
Butene amines	C_4H_9N	72.0808	0.013	0.015	0.010
Nitroethene	$C_2H_3NO_2$	74.0237	0.065	0.096	0.102
C_3 amides	C_3H_7NO	74.06	0.121	0.321	0.324
Nitroethane	$C_2H_5NO_2$	76.0393	0.052	0.083	0.088
Pyridine, C_5 nitriles	C_5H_5N	80.05	0.034	0.072	0.086
Methyl pyrrole	C_5H_7N	82.065	0.022	0.016	0.013
C_5 nitrile	C_5H_9N	84.081	0.038	0.040	0.037
Nitropropanes	$C_3H_7NO_2$	90.055	0.027	0.060	0.060
C_6 nitrile	$C_6H_{11}N$	98.096	0.008	0.010	0.004
Benzonitrile	C_7H_5N	104.049	0.009	0.026	0.032
Toluidine	C_7H_9N	108.081	0.043	0.117	0.111
C_9 aromatic nitrile	C_9H_9N	132.081	0.012	0.006	0.007
Nitrotoluene	$C_7H_7NO_2$	138.055	0.005	0.006	0.008
Nitrophenol	$C_6H_5NO_3$*	140.034	0.006	0.022	0.028
Methyl nitrophenols	$C_7H_7NO_3$*	154.05	0.007	0.033	0.044
C_{11} aromatic nitrile	$C_{11}H_{13}N$	160.112	0.004	0.007	0.005
C_3 nitrophenols	$C_9H_{11}NO_3$*	182.081	0.003	0.006	0.006

* These species were input into the model simulation.

Table S3. The canister VOC species measured by GC-MS/FID/ECD constrained in model simulation.

No.	VOC species	No.	VOC species
1	Ethane	20	Propene
2	Propane	21	i-Butene
3	i-Butane	22	1-Butene
4	n-Butane	23	1,3-butadiene
5	i-Pentane	24	2-Methyl-1-Butene
6	n-Pentane	25	3-Methyl-1-Butene
7	2,2-Dimethylbutane	26	2-Methyl-2-Butene
8	2,3-Dimethylbutane	27	1-Pentene
9	2-Methylpentane	28	trans-2-Pentene
10	3-Methylpentane	29	cis-2-Pentene
11	n-Hexane	30	Ethyne
12	2-Methylhexane	31	Methyl nitrate
13	3-Methylhexane	32	Ethyl nitrate
14	n-Heptane	33	i-Propyl nitrate
15	n-Octane	34	n-Propyl nitrate
16	n-Nonane	35	2-Butyl nitrate
17	n-Decane	36	3-Methyl-2-butyl nitrate
18	Cyclohexane	37	2-Pentyl nitrate
19	Ethene	38	3-Pentyl nitrate

Table S4. The classification of observed VOC subgroups in RIR calculation.

Subgroup	Number of species	Species in MCM
BVOCs	3	C5H8, APINENE, BPINENE
AVOCs	45	C2H6, C3H8, IC4H10, NC4H10, IC5H12, NC5H12, M22C4, M23C4, M2PE, M3PE, NC6H14, M2HEX, M3HEX, NC7H16, NC8H18, NC9H20, NC10H22, CHEX, C2H4, C3H6, MEPROPENE, BUT1ENE, C4H6, ME2BUT1ENE, ME3BUT1ENE, ME2BUT2ENE, PENT1ENE, TPENT2ENE, CPENT2ENE, C2H2, BENZENE, TOLUENE, STYRENE, OXYL, MXYL, PXYL, EBENZ, IPBENZ, PBENZ, METHTOL, PETHTOL, TM135B, OETHTOL, TM124B, TM123B

OVOCs	63	CH3OH, CH3CHO, ACR, CH3COCH3, MVK, MACR, C4ALDB, MEK, C3H7CHO, IPRCHO, C4H9CHO, PHENOL, CYHEXONE, C5H11CHO, HEX2ONE, HEX3ONE, BENZAL, CRESOL, C6H13CHO, OXYLAL, MXYLAL, PXYLAL, EBENZOL, PXYLOL, MXYLOL, OXYLOL, TM135BZOL, TM123BOL, TM124OL, METOH, PETOH, OETOH, NOPINONE, HCOOH, CH3CO2H, HOCH2CHO, ETHGLY, MGLYOX, ACO2H, ACETOL, PROPACID, PROPGLY, BZFUONE, BIACET, MACO2H, BUTACID, PXYFUONE, TLFUONE, CO2C43CHO, PENTACID, CATECHOL, EBFUONE, OXYFUONE, MXYFUONE, TMB1FUONE, CO25C6, PXYLCO2H, MXYLCO2H, OXYLCO2H, CH3CO3H, MALANHY, METHCOACET, MMALANHY

Table S5. Observed and model simulated daytime average concentrations of selected OVOC species (methanol, acetaldehyde, and acetone) and the underestimation fraction of simulation in early winter.

OVOC species	Observed daytime concentration (ppbv)	Simulated daytime concentration (ppbv)	Underestimation of simulation (%)
Methanol	10.32	0.09	99.2
Acetaldehyde	4.07	0.33	91.8
Acetone	6.28	1.67	73.4

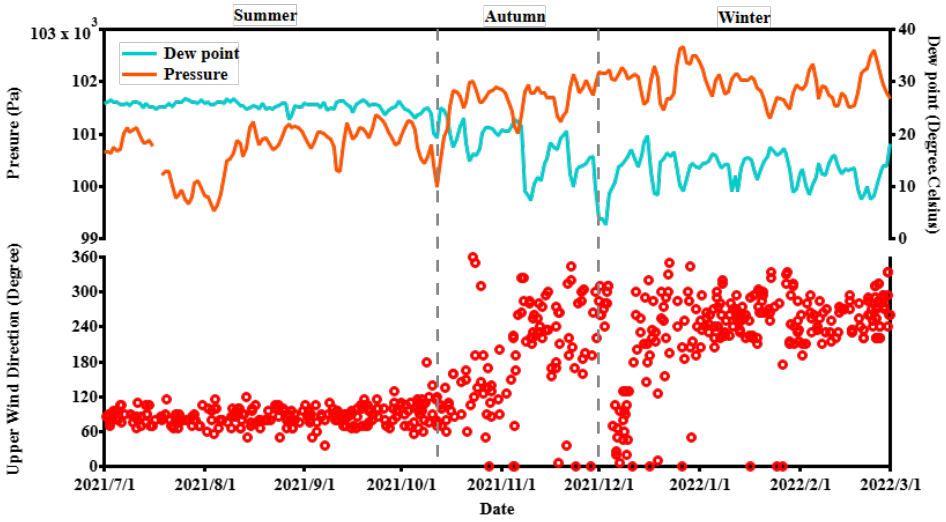

Figure S1. Temporal variation of upper-level wind direction, sea level pressure and dew point in Hong Kong measured by Hong Kong Observatory Station from July 2021 to March 2022. The seasonal transition from summer to early winter was characterized by a rapid shift from high dew point and low sea-level pressure to cold and high-pressure systems, accompanied by a change in upper-level wind direction from easterly/southeasterly to westerly/northwesterly (Li et al., 2016; Wong et al., 2022).

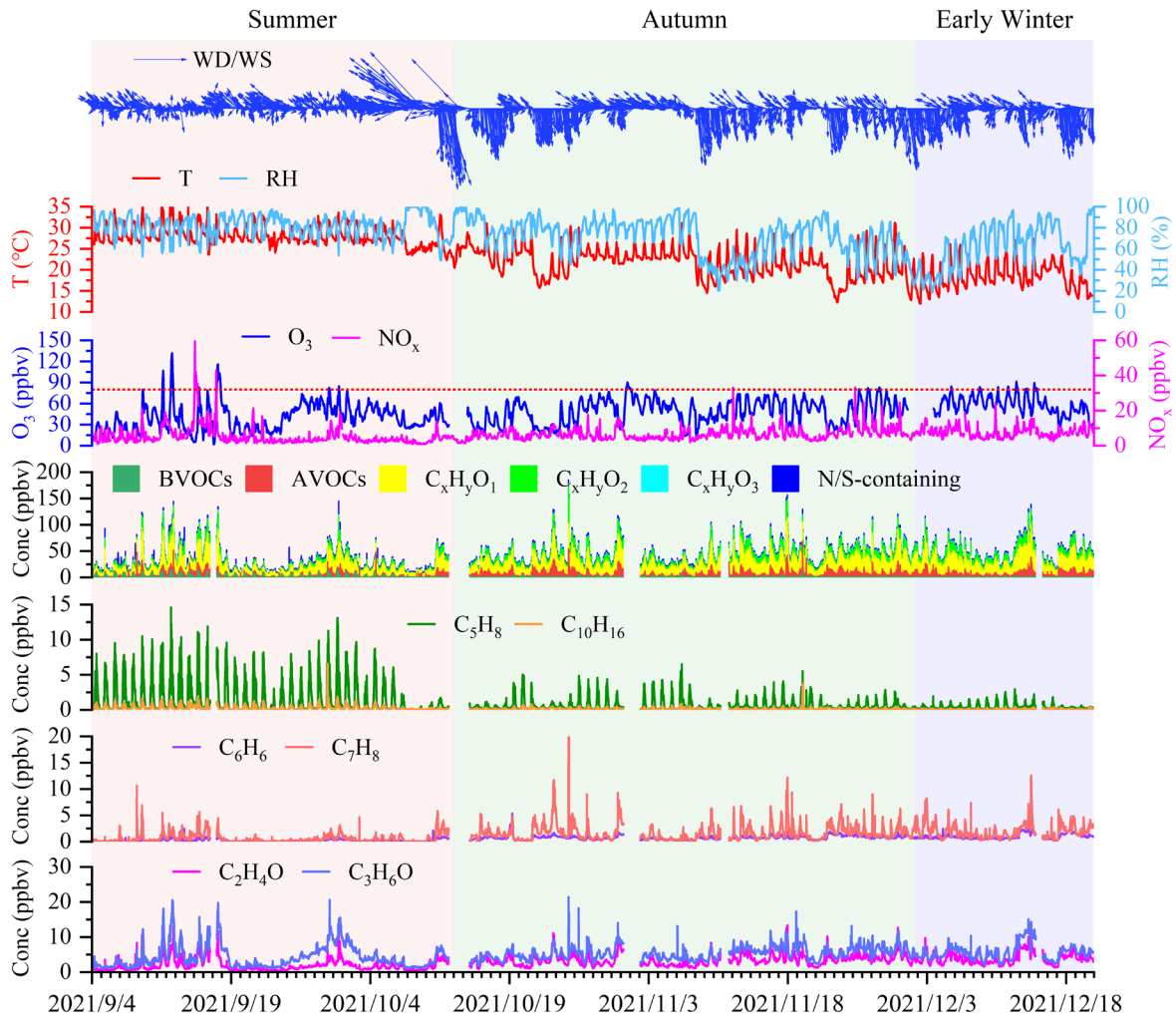

Figure S2. Time series of meteorological parameters (T, RH, wind direction and wind speed), trace gases (O_3, NO_x), VOC groups measured by PTR-ToF-MS, and representative species from September 4 to December 20 in 2021 in Hong Kong. The red dash line represents the O_3 concentration of about 80 ppbv. The shaded areas in orange, green, and violet colors represent summer, autumn, and early winter, respectively.

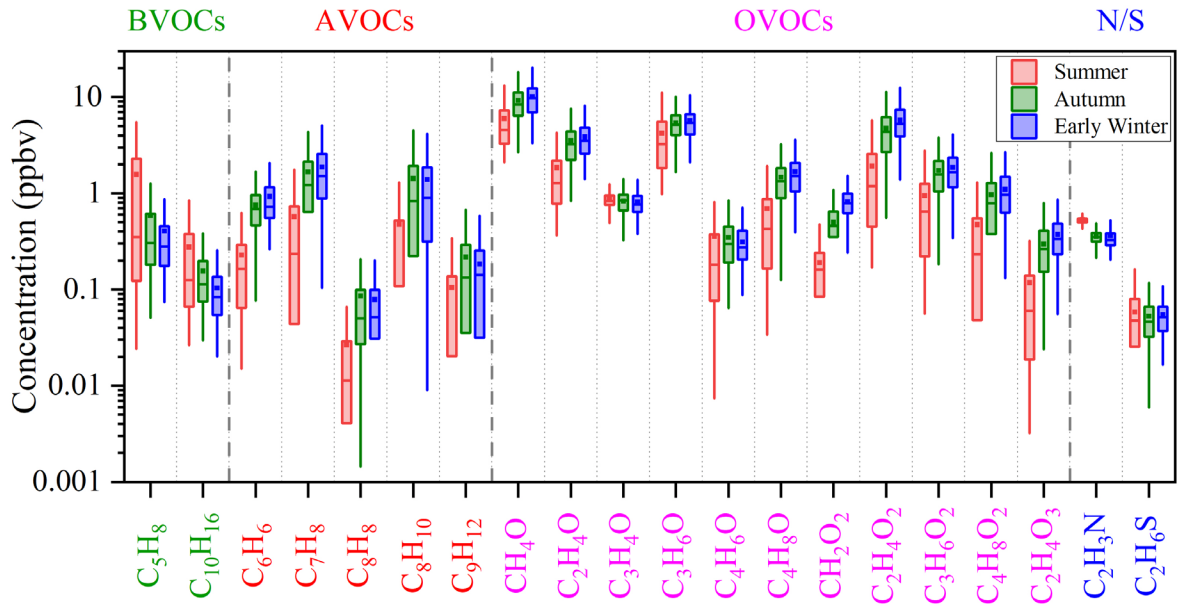

Figure S3. The concentration comparison of key species of different VOC groups in summer, autumn, and early winter.

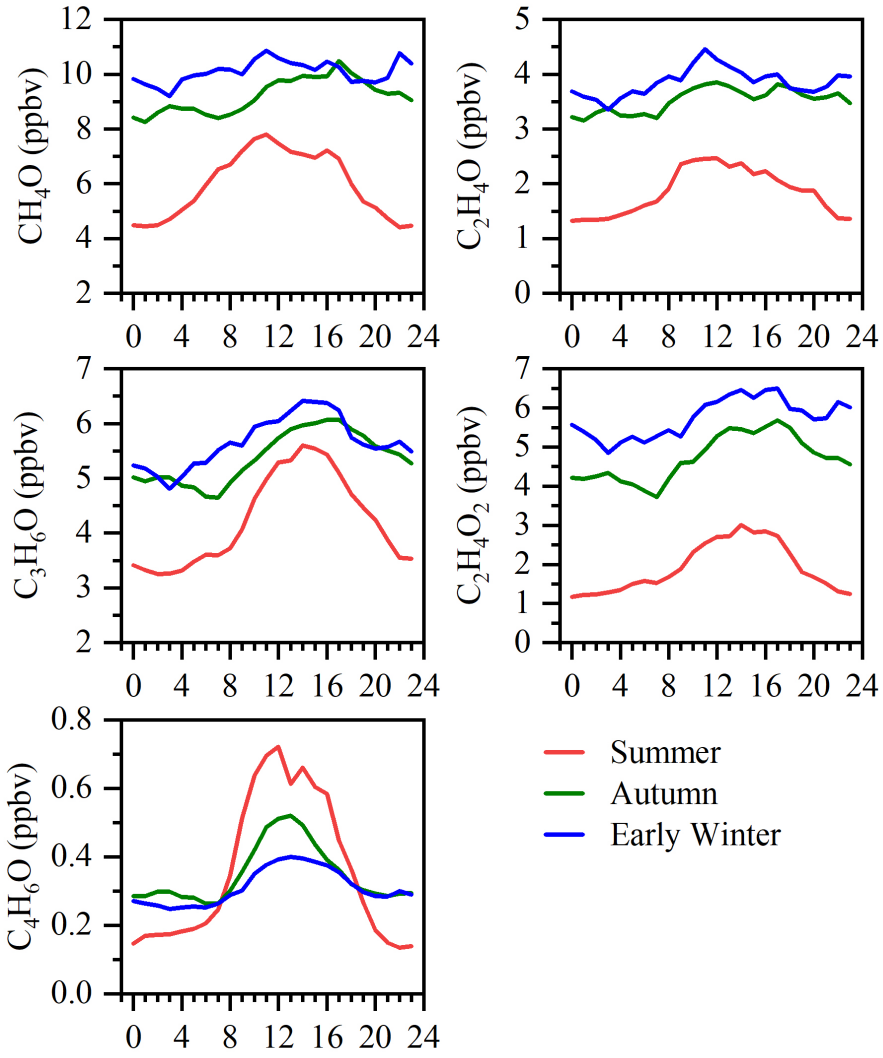

Figure S4. Diurnal patterns of specific OVOC species including CH_4O, C_2H_4O, C_3H_6O, $C_2H_4O_2$, and C_4H_6O in summer, autumn, and early winter.

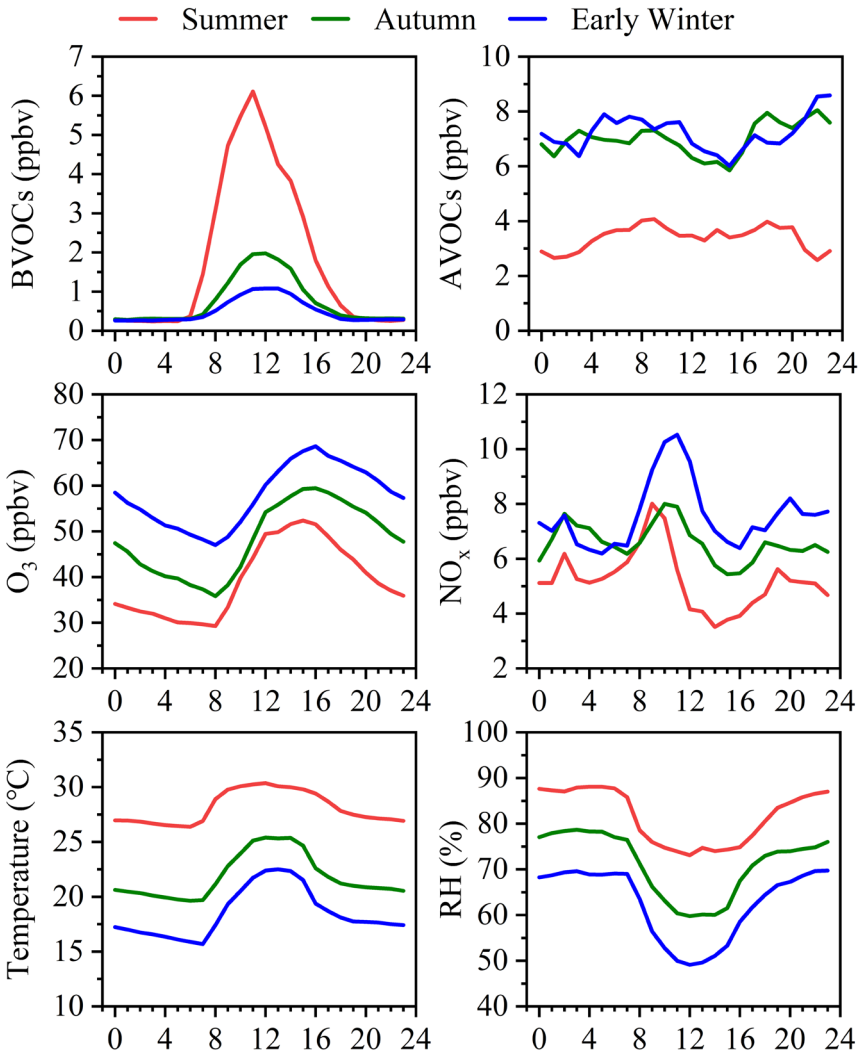

Figure S5. Diurnal patterns of BVOCs, AVOCs, trace gases (O_3 and NO_x), and meteorological parameters (temperature and RH) in summer, autumn, and early winter.

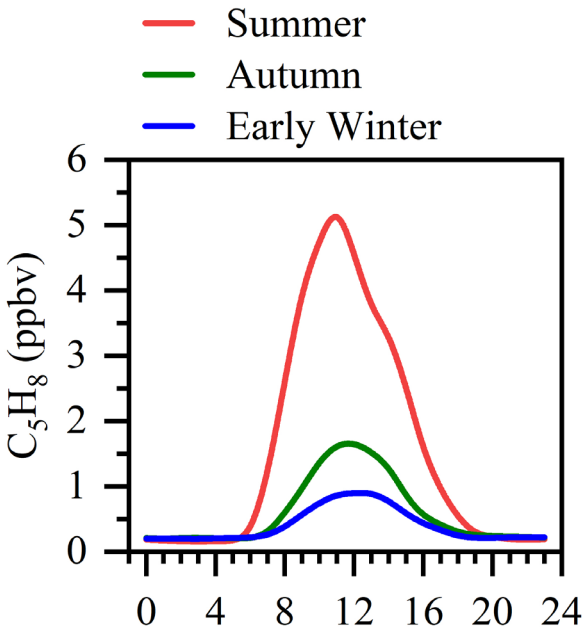

Figure S6. Diurnal pattern of C_5H_8 in summer, autumn, and early winter.

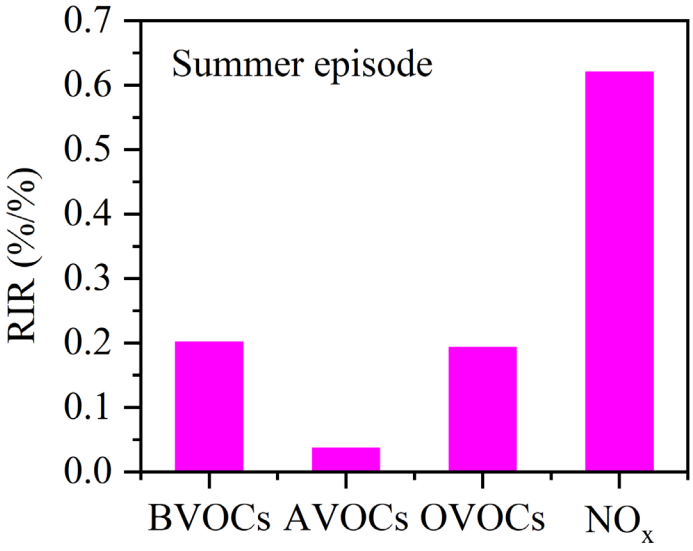

Figure S7. Average RIR values of O_3 precursors (observed BVOCs, AVOCs, OVOCs, and NO_x) in summer episode.

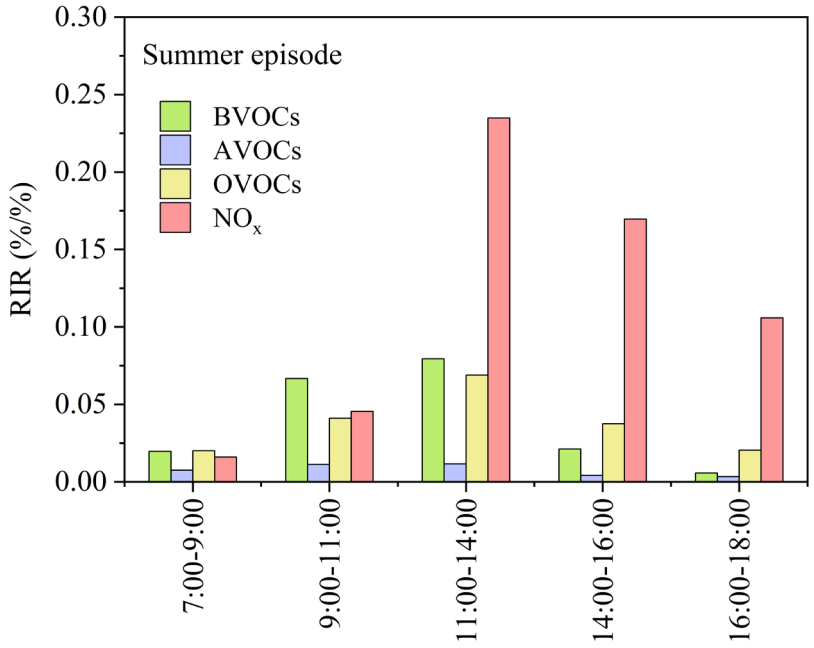

Figure S8. Diurnal patterns of RIR values of O_3 precursors in summer episode.

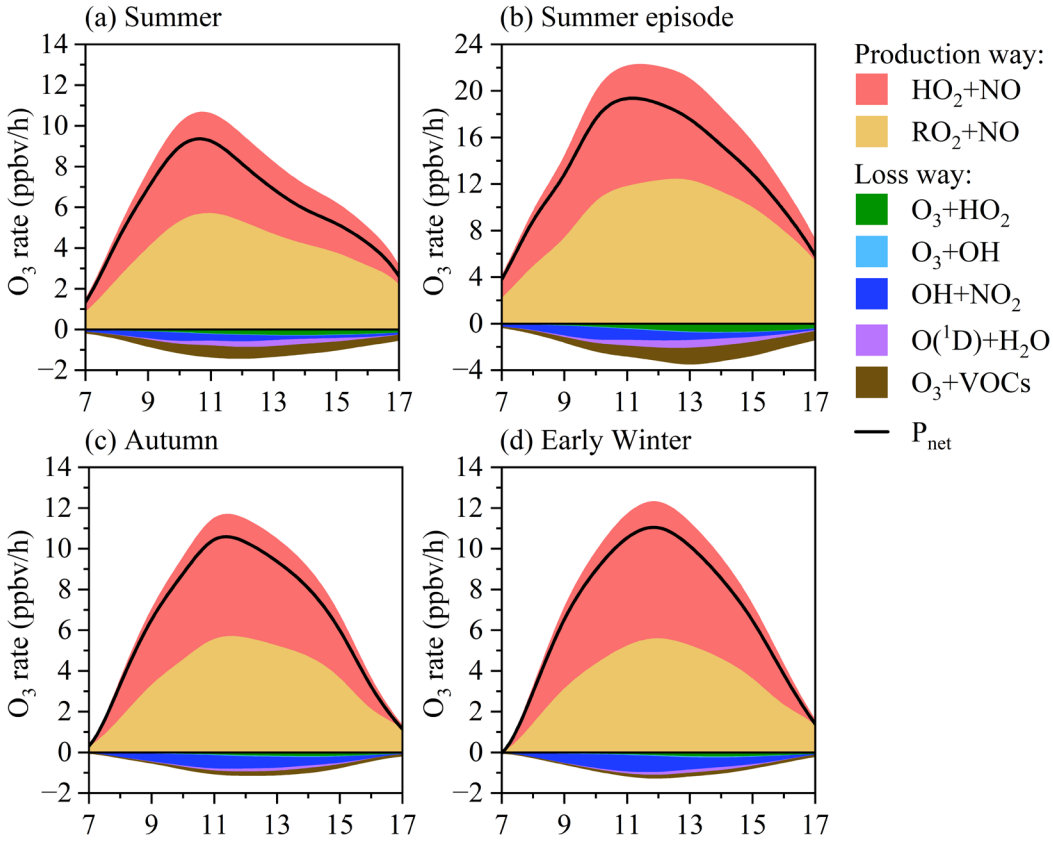

Figure S9. Model simulated daytime O_3 production and loss rates of main pathways in (a) summer, (b) summer episode, (c) autumn, and (d) early winter. The net O_3 production rate (P_{net}) is the black line.

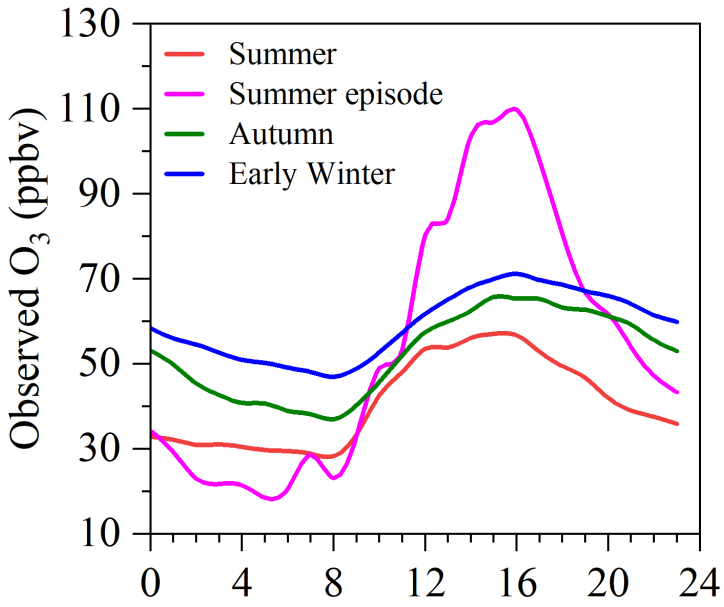

Figure S10. Diurnal patterns of observed O_3 concentration in summer, summer episode, autumn, and early winter.

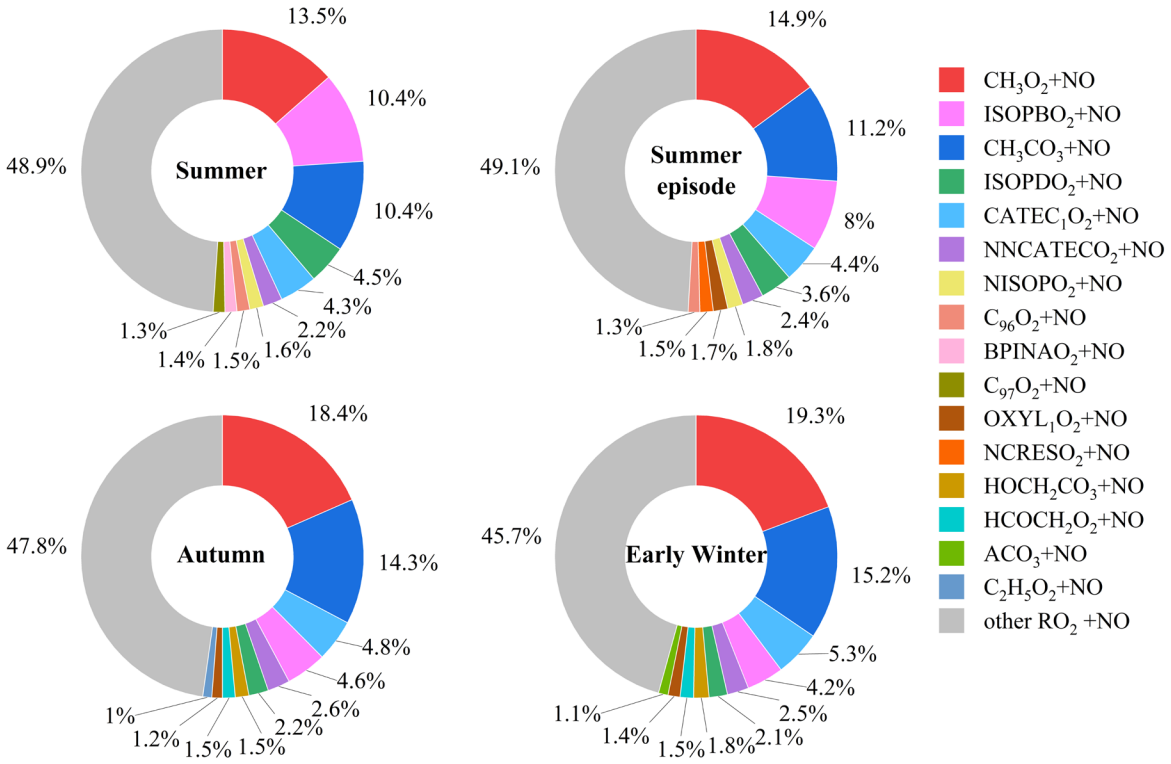

Figure S11. The contributions of top ten pathways of RO_2 + NO towards daytime O_3 formation in summer, summer episode, autumn, and early winter.

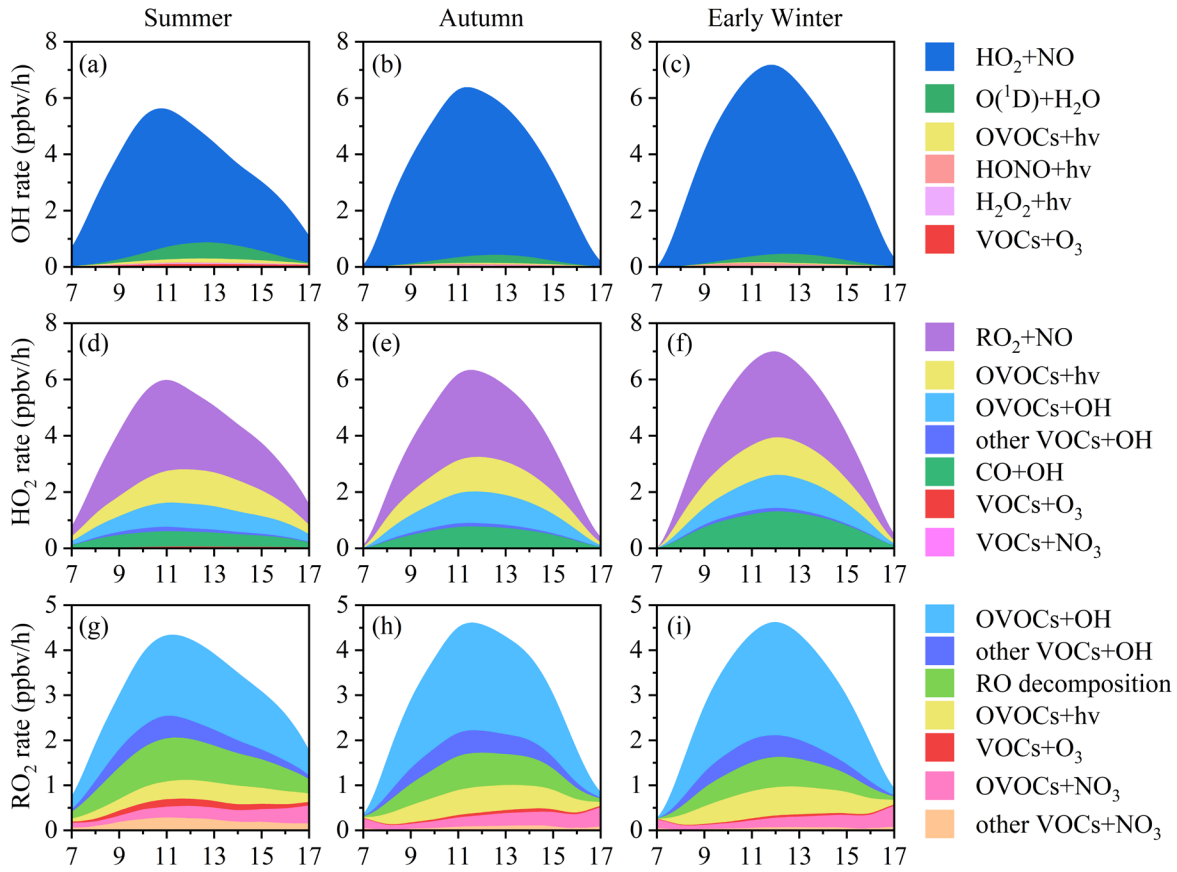

Figure S12. Model simulated daytime production rates of OH, HO_2 and RO_2 radicals of main pathways in summer, autumn, and early winter.

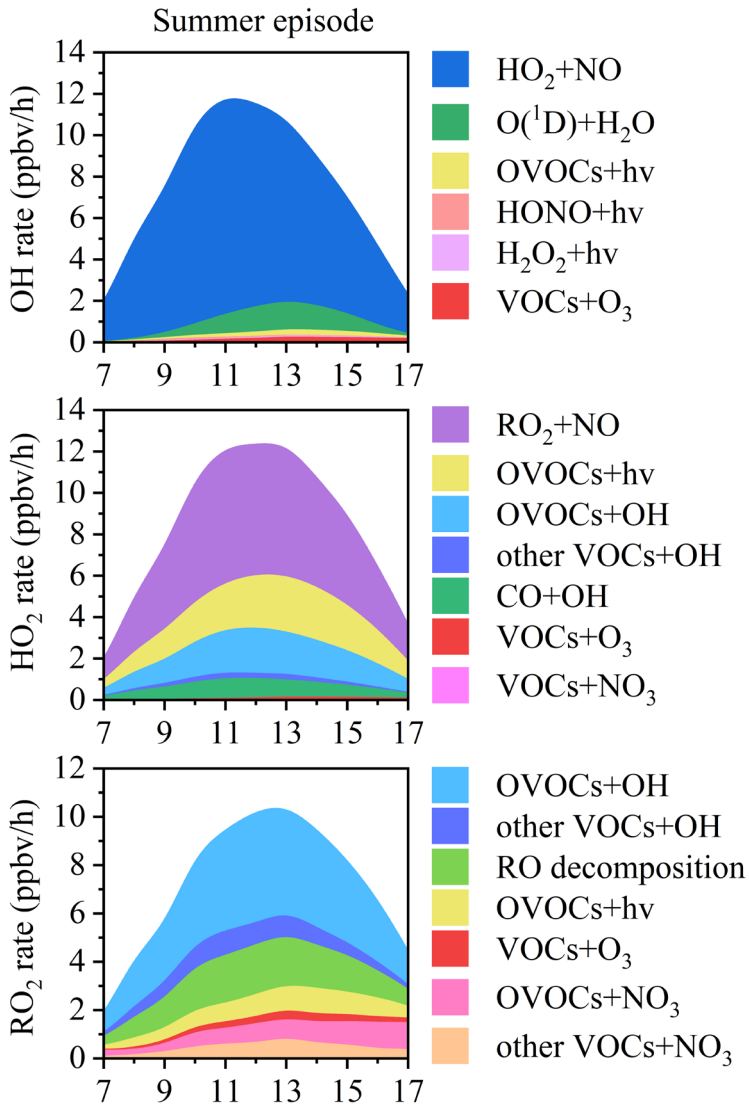

Figure S13. Model simulated daytime production rates of OH, HO_2 and RO_2 radicals of main pathways in summer episode.

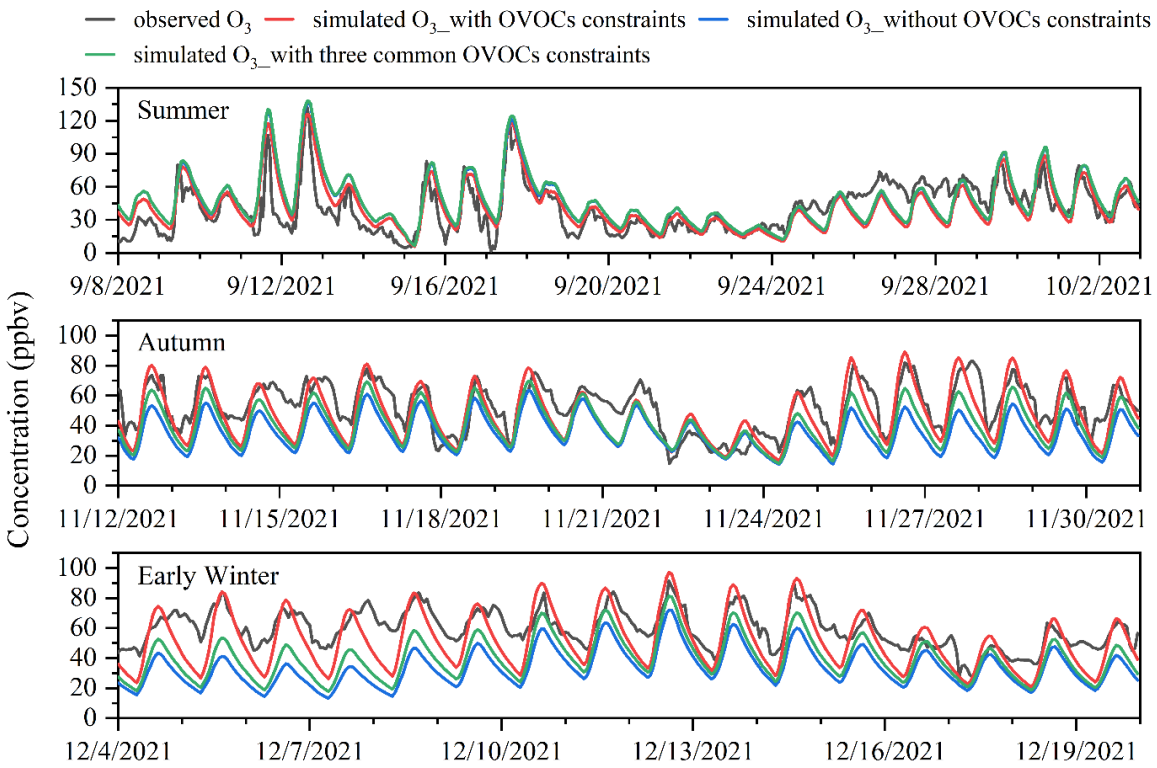

Figure S14. Comparison between the observed O_3 and simulated O_3 concentration with all observed OVOCs, with three common OVOCs (i.e., methanol, acetaldehyde, acetone), and without OVOCs constraints in summer, autumn, and early winter.

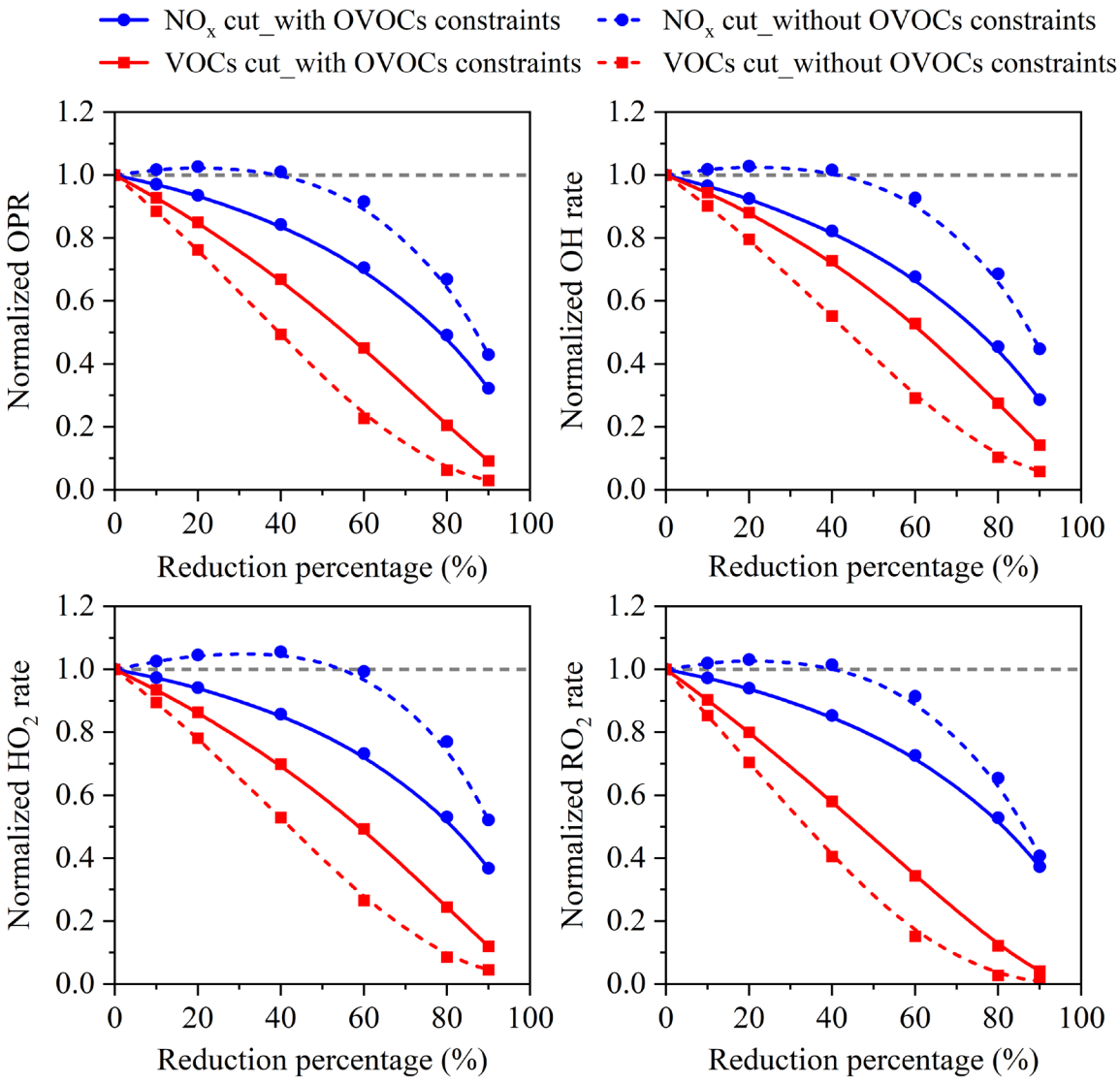

Figure S15. Changes in daytime production rate of O_3 (OPR), OH radical, HO_2 radical, and RO_2 radicals with the reduction of VOCs or NO_x from 0% to 90% with and without observed OVOCs constraints. The daytime production rates were normalized to the corresponding values in the base run. The grey dash line represents the normalized production rate of 1.0, indicating no production rate changing.

References:

Li, Z., Lau, W. K. M., Ramanathan, V., Wu, G., Ding, Y., Manoj, M. G., Liu, J., Qian, Y., Li, J., Zhou, T., Fan, J., Rosenfeld, D., Ming, Y., Wang, Y., Huang, J., Wang, B., Xu, X., Lee, S. S., Cribb, M., Zhang, F., Yang, X., Zhao, C., Takemura, T., Wang, K., Xia, X., Yin, Y., Zhang, H., Guo, J., Zhai, P. M., Sugimoto, N., Babu, S. S., and Brasseur, G. P.: Aerosol and monsoon climate interactions over Asia, Reviews of Geophysics, 54, 866-929, 10.1002/2015rg000500, 2016.

Wong, Y. K., Liu, K. M., Yeung, C., Leung, K. K. M., and Yu, J. Z.: Measurement report: Characterization and source apportionment of coarse particulate matter in Hong Kong: insights into the constituents of unidentified mass and source origins in a coastal city in southern China, Atmos. Chem. Phys., 22, 5017-5031, 10.5194/acp-22-5017-2022, 2022.